ISCI, Volume *21*

Supplemental Information

Tracking Dynamics of Spontaneous Tumors in Mice Using Photon-Counting Computed Tomography

Franca Cassol, Loriane Portal, Sylvie Richelme, Mathieu Dupont, Yannick Boursier, Maria Arechederra, Nathalie Auphan-Anezin, Lionel Chasson, Caroline Laprie, Samantha Fernandez, Laure Balasse, Fabienne Lamballe, Rosanna Dono, Benjamin Guillet, Toby Lawrence, Christian Morel, and Flavio Maina

SUPPLEMENTAL INFORMATION

SUPPLEMENTAL MATERIALS

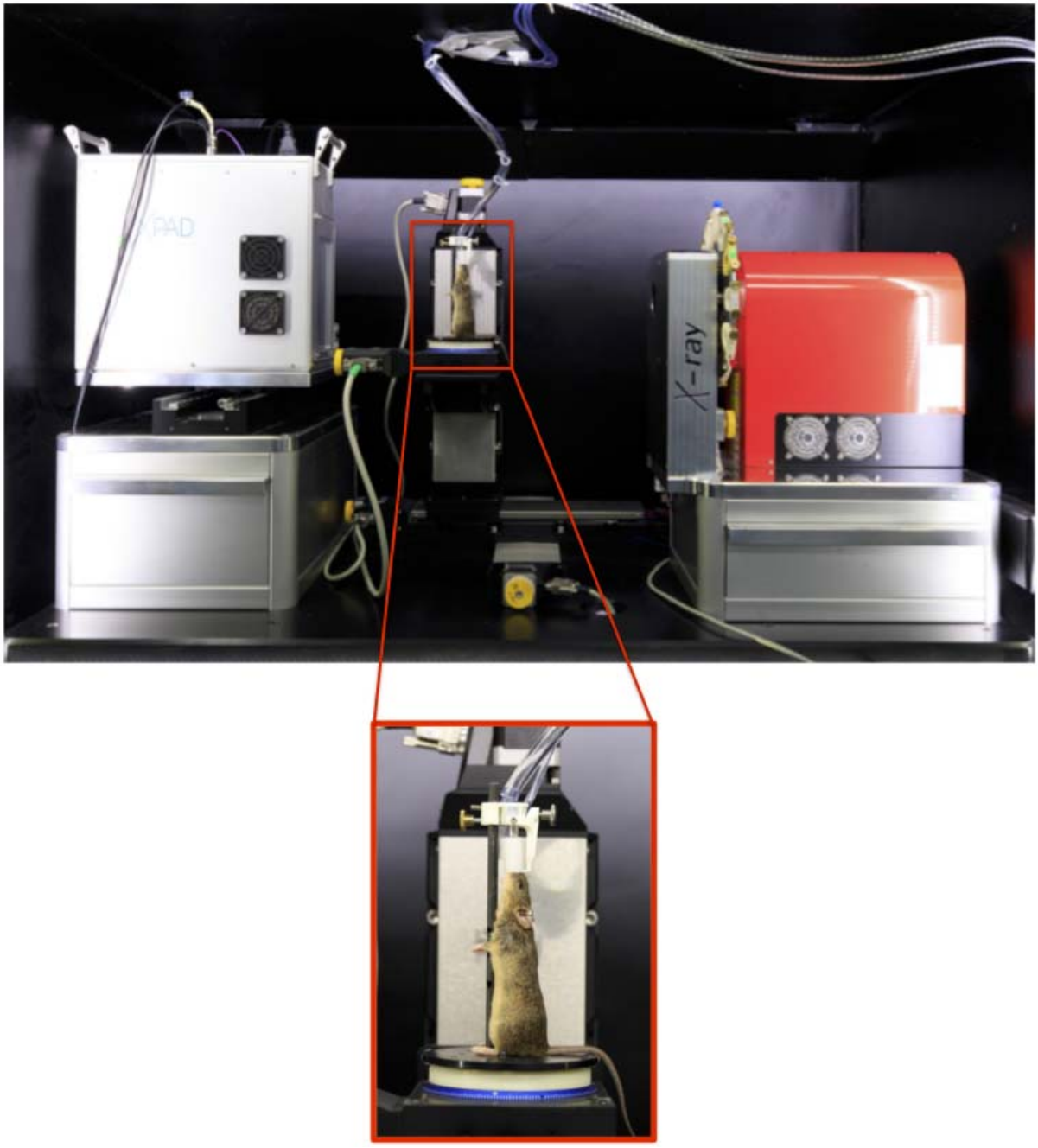

Figure S1. Photography of the PIXSCAN-FLI PC-CT prototype equipped with a XPAD3/Si hybrid pixel camera (top) showing the position of mice during recoding (bottom), Related to Figure 1.

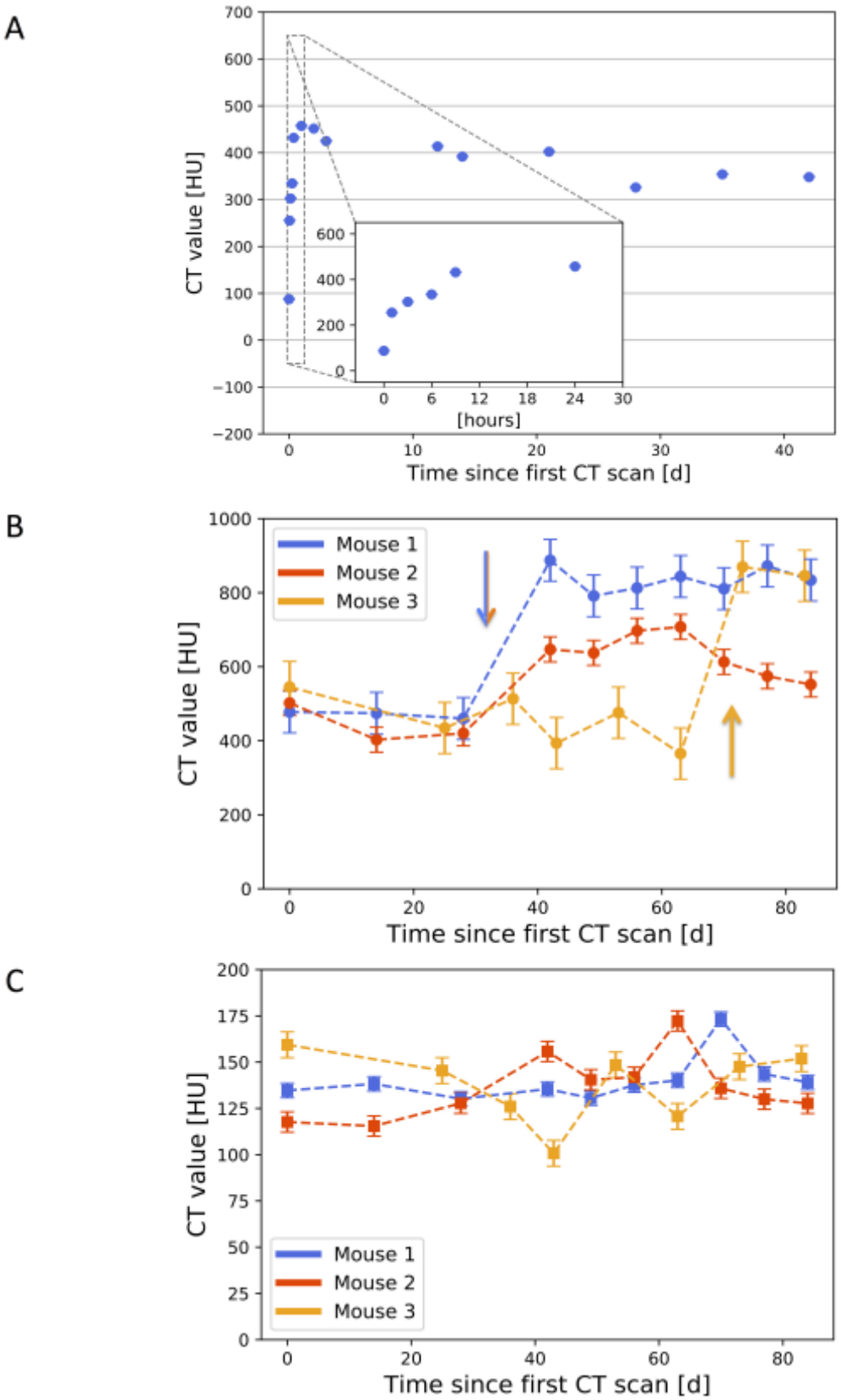

Figure S2. Graphs reporting CT values in livers and tumors, Related to Figure 1. (A) Graph reporting the fast increase of the liver CT value (in Hounsfield units) after injection of 4 µL/g mouse of

ExiTron^{TM} nano 12000. (B, C) Graphs reporting longitudinal monitoring of the CT value (in Hounsfield units) in the liver (B) and in the tumor region (C) for three representative mice. We observed a contrast deviation in livers after a second injection of the ExiTron^{TM} nano 12000 (indicated by arrows), coherent with an additional accumulation of the contrast agent in Kupffer cells. Instead, the tumor contrast was stable overtime, and no significant variations were observed.

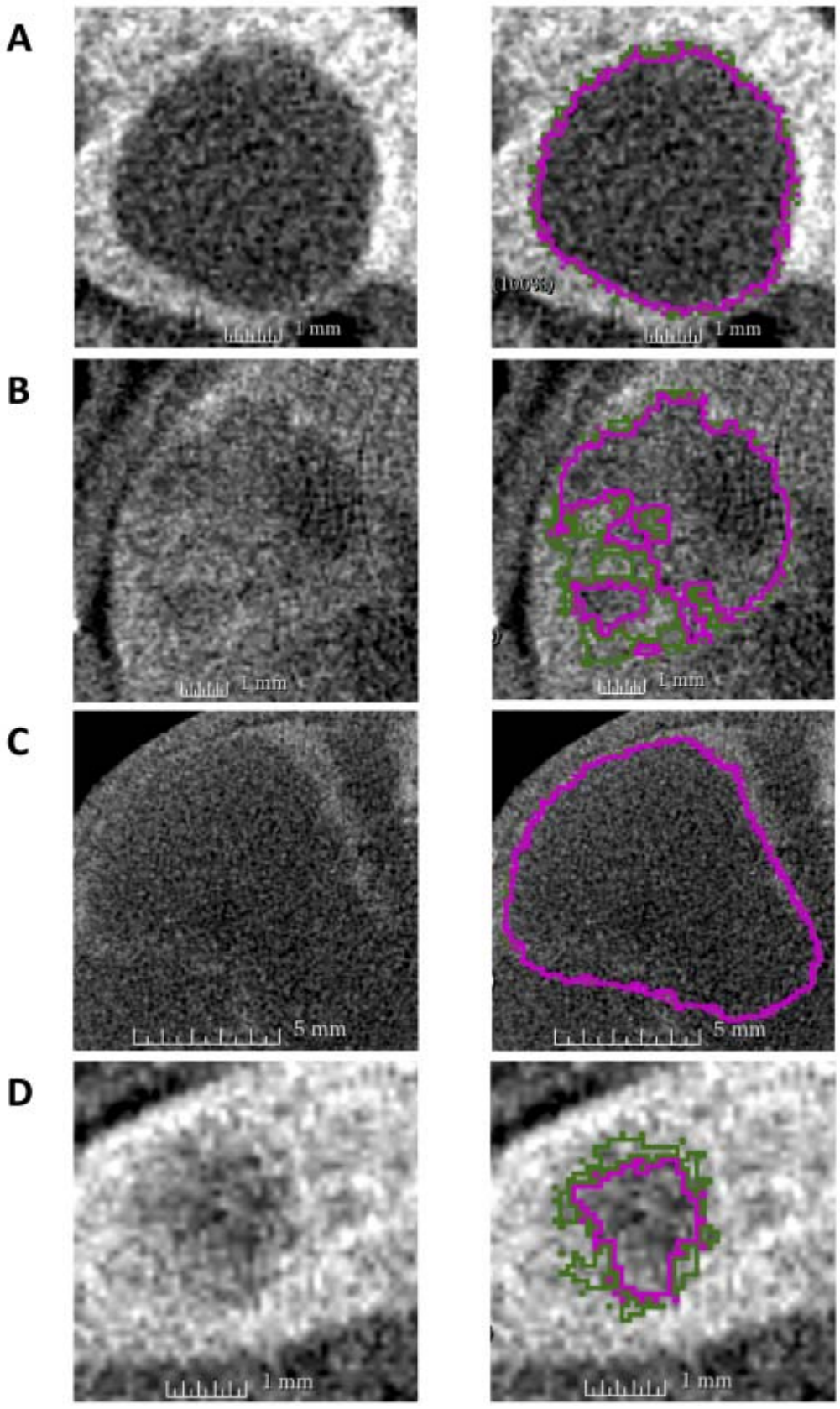

Figure S3. Panels correspond to transverse slices at the tumor maximal diameter, Related to Figure 2. Images were acquired at D49 (A and D), D21 (B), and D15 (C), and are also reported in

Figure 2G-J. Images are reported without (left) and with the two-contrast thresholds applied (right). Tumor volume measurements are shown for the 2 defined contrast thresholds: $Th_{0.50}$ (pink) and $Th_{0.75}$ (green).

cohorts	tumor	mouse	ID	follow-up time (days)	% of tumor regression after treatment
1° cohort	M1-T1	M1	672 472	84	
	M1-T2				
	M1-T3				
	M1-T4				
	M2-T1	M2	672 399	77	
	M2-T2				
	M2-T3				
	M2-T4				
	M3-T1	M3	670 320	77	
	M3-T2				
	M4-T1	M4	672 524	28	
	M4-T2				
	M5-T1	M5	672 526	42	
	M5-T2				
	M6-T1	M6	672 403	71	
2° cohort	M7-T1	M7	672 517	70	100%
	M7-T2				92%
	M8-T1	M8	673 823	70	99%
	M9-T1	M9	673 822	70	96%
	M10-T1	M10	672 398	70	21%
	M11-T1	M11	672 536	28 (D)	75% (at 20 days)
	M12-T1	M12	673 830	34 (D)	23% (at 30 days)
3° cohort		M13	674 670	15	
		M14	673 598	15	
		M15	673 486	15	

Table S1. Table summarizing the tumors and the corresponding mice used for longitudinal PC-CT imaging, Related to Figure 1. Mice found dead (FD) during the manipulation are indicated. The percentage of tumor regression in the cohort of treated mice is reported. For mice found dead (M11 and M12), the percentage of tumor regression correspond to the last imaging analysis performed.

mouse	genotype	untreated/treated	case	sample	histological description	diagnosis
674638	*Alb-R26^{Met}*	untreated	19-0171	liver	Normal lobular architectecture	
674642	*Alb-R26^{Met}*	untreated	19-0172	liver	Normal lobular architectecture	
674712	*Alb-R26^{Met}*	untreated	19-0174	liver	Normal lobular architectecture	
674711	*Alb-R26^{Met}*	untreated	19-0173	tumor T1	Focal ill-defined nodular hepatocytic proliferative foci with loss of lobular architecture and locally infiltrative growth (carcinoma)	Hepatocytic carcinoma, well differentiated
674749	*Alb-R26^{Met}*	untreated	19-0176	tumor T2	Focal well-defined, expansile, nodular hepatocytic proliferative foci with loss of lobular architecture	Hepatocytic adenoma
674754	*Alb-R26^{Met}*	untreated	19-0177	tumor T1	Focal well-defined, expansile, nodular hepatocytic proliferative foci with loss of lobular architecture	Hepatocytic adenoma
			19-0178	tumor T1C	Focal ill-defined nodular hepatocytic proliferative foci with loss of lobular architecture and locally infiltrative growth (carcinoma)	Hepatocytic carcinoma, well differentiated
			19-0179	tumor T3	Focal well-defined, expansile, nodular hepatocytic proliferative foci with loss of lobular architecture	Hepatocytic adenoma
674763	*Alb-R26^{Met}*	untreated	19-0181	tumor T1	Focal well-defined, expansile, nodular hepatocytic proliferative foci with loss of lobular architecture	Hepatocytic adenoma
			19-0182	tumor T2	Focal well-defined, expansile, nodular hepatocytic proliferative foci with loss of lobular architecture	Hepatocytic adenoma
673486	*Alb-R26^{Met}*	treated with MEK+BCL-XL inhibitors	18-0668	tumor T1A	Focal nodular hepatocytic proliferative foci with loss of lobular architecture (adenoma). Multifocal Kupffer cell hyperplasia	Hepatocytic adenoma, multifocal necrosis

			18-0671	tumor T3B	Localized proliferation of hepatocytes, phenotypically similar to adjacent hepatocytes without persistent lobular architecture (no visible portal tracts) : adenoma Kupffer cell hypertrophy	Hepatocytic adenoma
			18-0672	liver	Normal. Mild vacuolar centrolobular degeneration Kupffer cells hypertrophy	
673598	*Alb-R26^{Met}*	treated with MEK+BCL-XL inhibitors	18-0670	liver C	Normal lobular architecture Focal marked Kupffer cell hypertrophy and hyperplasia with enlarged cells	Focal marked Kupffer cells hyperplasia (with abundant intracellular material)
			18-0669	tumor T1A	Medio and centrobular hypertrophy with karyomegaly, mild Kupffer cell hypertrophy	
674670	*Alb-R26^{Met}*	treated with MEK+BCL-XL inhibitors	18-0665	liver C	Normal lobular architectecture	
			18-0666	tumor T1C	Well delineated hepatic nodule, locally infiltrating the adjacent parenchyma Loss of normal lobular architecture Well differentiated hepatocytes, forming trabeculae Focal necrotic foci (1x0.5 mm) Peritumoral Kupffer cells hyperplasia	Hepatocarcinoma, well differentiated, locally necrotic Peritumoral kupffer cell hyperplasia

Table S2. Table summarizing the mice used for histological studies, Related to Figure 9.

TRANSPARENT METHODS

Ethics Statement. All procedures with animals were performed in accordance with the European Community Council Directive of 22 September 2010 on the protection of animals used for experimental purposes (2010/63/EU). The experimental protocols were carried out in compliance with institutional Ethical Committee guidelines for animal research (comité d'éthique pour l'expérimentation animale – Comité d'éthique de Marseille) and in compliance with French law, under an agreement number E1305521, Ministère de l'enseignement supérieur de la recherche et de l'innovation. Mice were kept in a dedicated pathogen free facility, with a light/dark cycle, and in cages with an enrichment environment. Mice received Safe Complete Care Competence (SAFE A04) as complete aliment *ad libitum*. The project authorization of Maina laboratory is: APAFIS #8214-2016121417291352.v5 delivered by the "Ministère de l'Enseignement Supérieur, de la Recherche et de l'Innovation".

Alb-R26^{Met} **mice.** The generation of the *R26^{stopMet}* mice (international nomenclature *Gt(ROSA)26Sor$^{tm1(Actb-Met)Fmai}$*) carrying a conditional mouse-human chimeric *Met* transgene into the *Rosa26* locus, and the genotyping procedures were previously reported (Fan et al., 2015; Genestine et al., 2011; Tonges et al., 2011). The mouse line expressing Cre recombinase under the *Alb* promoter (*B6.Cg-Tg(Alb-cre)21Mgn/J*) was obtained from the Jackson Laboratory. *Alb-R26^{Met}* mice were generated by crossing the *R26^{stopMet}* and *Alb-R26^{Met}* mice (Arechederra et al., 2018; Fan et al., 2017; Fan et al., 2019). Mice were maintained in a 50% mixed background of 129/SV and C57BL6, and genotyped by PCR analysis of genomic DNA as previously reported (Fan et al., 2015; Genestine et al., 2011). Only males were used for these studies. From a total of 41 mice aged between 58 and 68 weeks at the first PC-CT imaging analysis, 15 mice with one or multiple liver tumors were used for these studies (Table S1). This number of mice was chosen to support our studies with several tumors from independent animals while respecting ethical recommendations to limit the number of mice for experimental manipulations.

PIXSCAN-FLI PC-CT prototype. The PC-CT PIXSCAN-FLI prototype (Figure S1) is contained in a lead/steel box of dimensions 139.5 cm × 101 cm × 99.5 cm (L × W × H). It is composed of a tungsten

anode X-ray tube Microfocus L12161-07 (Hamamatsu Photonics K.K., Japan) with a 7-50 µm emission spot and a hybrid pixel camera XPAD3 with pixels of 130 µm × 130 µm (Cassol et al., 2009; Pangaud et al., 2007). In front of the X-ray tube, a wheel holding filters of different materials (Al, Cu, Ag, Mo and others) and thicknesses permits further modulation of the cone beam of X-rays. The X-ray camera XPAD3 is composed of eight contiguous horizontal modules slightly tilted vertically and overlapped to avoid dead areas. Each module has a size of 7.5 cm × 1.6 cm and consists of a 500 µm thick Si sensor with 67,200 (560 × 120) pixels of 130 µm × 130 µm bump-bonded to seven chips XPAD3, each of which reading out a matrix of 9,600 (80 × 120) pixels. Thus, the camera has a sensitive surface of 7.5 cm × 11.5 cm and a total of 537,600 pixel. For in vivo imaging, the mouse was placed vertically between the X-ray source and the XPAD3 camera on a rotating platform positioned on a (*x*,*y*,*z*) translation table, as shown in Figure S1. For this study, the platform rotation axis distance from the camera was set to 39 cm, which corresponds to an imaging magnification factor of 1.54 due to the conical geometry of the beam. Tomographic scans were acquired under continuous rotation and continuous irradiation of X-rays generated with 50 kV and 500 µA (50 µm spot size) through 0.6 mm Al filtering, for which the camera detection efficiency amounts approximately to 35%. Mice were analyzed under general anesthesia (Isoflurane [~1.5 vol%]/O_2), which was controlled by a gas anesthesia unit (manufactured by Minerve; France). The dose rate at the mouse position was measured with a dosimeter Diados W 45-150 kV (PTW-Freiburg, Germany). The dose per scan delivered to the mouse was estimated by multiplying the dose rate by the scan duration.

Data processing. Tomographic scans of 720 projections with a 0.5° step, thus covering a full rotation, have been acquired. Spurious measurements (photon counts per pixel) due to dead or miscalibrated pixels, usually less than 2% of the total number of pixels, were detected using the prior acquisition and the processing of 25 dark fields and 25 flat fields. Missing data are recovered by linear interpolation based on the three closest neighbors given by a Voronoï tessellation calculated from the position in three dimensions of the pixels, which encompasses the specific internal tiled geometry of the XPAD3 camera and the global geometric configuration of the PIXSCAN-FLI prototype.

In particular, the geometry of the imaging setup was estimated beforehand through a dedicated minimization procedure based on the scan of rotating steel balls (Khoury et al., 2009). Each projection

was normalized by the mean of the 25 flat fields. The negative logarithm of the results constituting the tomographic scans were first reconstructed with a standard FDK (Feldkamp et al., 1984) algorithm implemented with the standard Ram-Lak filter convolved without apodization in the spatial domain in the open source reconstruction toolkit OpenRTK (Rit et al., 2014) (https://www.openrtk.org/), which delivered volumes of size 588 x 882 x 588 with cubic pixels of size 0.084 mm defined by the cone beam magnification (1.54) of the 0.130 mm detector pixels. The reconstructed image spatial resolution of the system, which was estimated with a QRM-microCT-wire phantom (QRM, Germany), corresponds to a Point Spread Function (PSF) of about 0.125 mm FWHM. The voxel CT values (CTV) are expressed in Hounsfield units (HU) defined as $HU = 1000*(CTV - CTV_{water})/CTV_{water}$, where CTV_{water} is the CT value of a volume of water acquired under the same irradiation conditions. The reconstructed volumes were then analyzed with the 3D-Slicer software (https://www.slicer.org) to obtain a quantitative values of the tumor volume. This was achieved with a semiautomatic approach: a manual preliminary volume selection was followed by a reproducible volume quantification based on predefined contrast thresholds.

Principal Component Analysis (PCA) o screen data. For Principal Component Analysis (PCA), we revisited these *Alb-R26^{Met}* screen data: a) qPCR expression of 96 HCC markers (Fan et al., 2017), b) phosphokinome analysis of 23 signals (Fan et al., 2017), and c) methylome of CpG islands (Arechederra et al., 2018). PCA was performed using the Clustvis web tool: https://biit.cs.ut.ee/clustvis/.

In vivo drug administration in *Alb-R26^{Met}* mice. *Alb-R26^{Met}* mice carrying liver tumors were treated daily with intraperitoneal injections of drug combinations (ABT-737: 30 mg/kg; Selumetinib: 30 mg/kg). Concerning the 2° cohort, mice were treated for 40 days and imaging was performed every 10 days up to D70. Concerning the 3° cohort, mice were treated for 15 days, imaging was performed before starting the treatment and at D15. Livers and tumors were dissected and processed for histological analysis.

Histology and immunofluorescence microscopy. For histological analyses, tissues were fixed with 10% buffered formalin (VWR chemical, #9713.5000) for 24h, dehydrated and embedded in paraffin (Fischer histoplast, #6.774060), sectioned, stained with hematoxylin (Fischer, #6765004), and counterstained with eosin (Fischer, #10483750) using an automated Leica autostainer XL. The slides mounted with Entellan (Merck, #1.07961) were examined using a Nikon Eclipse. For immunofluorescent analysis, tissues were embedded in optimum cutting temperature medium (OCT) freezing media (Tissue-Tek, #4583). Consecutive liver sections were blocked for 1 hour in 2% BSA before overnight incubation with primary antibodies: anti-F4/80 (Bio-Rad, #MCA497-647; 1/200). Stained liver sections mounted in ProLong Gold antifade reagent with DAPI (Life Technologies, #P36931) were then analyzed by confocal microscopy using a Zeiss LSM 780. For cleaved Caspase-3 detection, sections were processed as previously reported (Furlan et al., 2012). Briefly, paraffin-embedded sections were deparaffinized, incubated for 20 minutes in epitope unmasking solution (Vector Laboratories), then permeabilized with PBS +0.5% Triton X-100 for 15 min. Endogenous peroxidase was quenched with 3% H_2O_2 in PBS +0.1% Triton X-100 for 15 min. Unspecific binding was then blocked with 10% BSA and 2% donkey serum for 1h at RT. Anti-cleaved Caspase-3 antibodies (Cell Signaling #9661, 1/250) were then applied overnight at 4°C. Endogenous biotin receptors present in livers were blocked by using the avidin-biotin blocking kit (Vector Laboratories). Secondary antibodies (biotinylated-donkey-anti-rabbit; 1/500) were then applied for 1h at RT. Signal amplification was performed using the VECTASTAIN®ABC-kit (Vector Labs).

SUPPLEMENTAL REFERENCES

Feldkamp, L.A., Davis, L.C., and Kress, J.W. (1984). Practical Cone-Beam Algorithm. J Opt Soc Am A *1*, 612-619.

Furlan, A., Lamballe, F., Stagni, V., Hussain, A., Richelme, S., Prodosmo, A., Moumen, A., Brun, C., Del Barco Barrantes, I., Arthur, J.S.*, et al.* (2012). Met acts through Abl to regulate p53 transcriptional outcomes and cell survival in the developing liver. J Hepatol *57*, 1292-1298.

Khoury, R., Bonissent, A., Clements, J.C., Meessen, C., Vigeolas, E., Billault, M., and Morel, C. (2009). A geometrical calibration method for the PIXSCAN micro-CT scanner. J Instrum *4*, P07016.

Rit, S., Oliva, M.V., Brousmiche, S., Labarbe, R., Sarrut, D., and Sharp, G.C. (2014). The Reconstruction Toolkit (RTK), an open-source cone-beam CT reconstruction toolkit based on the Insight Toolkit (ITK). J Phys Conf Ser *489*, 012079.